PHYSICAL REVIEW B **79**, 140510(R) (2009)

Raman phonons of α-FeTe and $Fe_{1.03}Se_{0.3}Te_{0.7}$ single crystals

T.-L. Xia,[1] D. Hou,[1,2] S. C. Zhao,[1] A. M. Zhang,[1] G. F. Chen,[3] J. L. Luo,[3] N. L. Wang,[3] J. H. Wei,[1] Z.-Y. Lu,[1] and Q. M. Zhang[1,4,*]

[1]*Department of Physics, Renmin University of China, Beijing 100872, People's Republic of China*

[2]*Department of Physics, Shandong University, Jinan 250100, People's Republic of China*

[3]*Beijing National Laboratory for Condensed Matter Physics, Institute of Physics, Chinese Academy of Sciences, Beijing 100190, People's Republic of China*

[4]*Department of Physics, Nanjing University, Nanjing 210093, People's Republic of China*

(Received 17 November 2008; revised manuscript received 17 March 2009; published 28 April 2009)

The polarized Raman-scattering spectra of nonsuperconducting α-FeTe and of As-free superconductor $Fe_{1.03}Se_{0.3}Te_{0.7}$ are measured at room temperature on single crystals. The phonon modes are assigned by combining symmetry analysis with first-principles calculations. In the parent compound α-FeTe, the A_{1g} mode of the Te atom and the B_{1g} mode of the Fe atom are observed clearly, while in superconducting $Fe_{1.03}Se_{0.3}Te_{0.7}$, only a softened Fe B_{1g} mode can be seen. No electron-phonon coupling feature can be distinguished in the spectra of the two samples. By contrast, the spectra of the superconducting system show a slight enhancement below 300 cm^{-1}, which may be of electronic origin.

DOI: 10.1103/PhysRevB.79.140510 PACS number(s): 74.25.Kc, 74.70.−b, 63.20.D−, 78.30.−j

The recent discovery of superconductivity in quaternary, rare-earth transition-metal oxypnictides, and especially the subsequent raising of the superconducting transition temperature (T_c) above the MacMillan limit has drawn great interest in the condensed-matter community.[1–5] *RE*$FeAsO_{1-x}F_x$, which we abbreviate as FeAs-1111, are superconductors showing such high-T_c values without copper-oxide planes. As such, it provides a system quite different from the cuprate superconductors in which to study the mechanism of high-temperature superconductivity. In rapid succession, Ba(Sr,Ca)K(Na)Fe_2As_2 (FeAs-122) (Refs. 6–10) and $Li_{1-x}FeAs$ (FeAs-111),[11–13] which has an infinite layered structure, were also found to be superconducting. It is thought that superconductivity in the FeAs-1111 and FeAs-122 series may have a direct connection to a spin-density-wave (SDW) anomaly occurring in the FeAs layer.[14] Superconductivity emerges when the SDW order is suppressed by chemical doping or by high pressures.

All these series of iron-based superconductors contain the element As, which is toxic on its own and would be even more so when oxidized to As_2O_3. As a substitute, α-FeSe with some Se deficiency, which is less toxic and easier to handle than arsenides, has also been found to exhibit superconductivity.[15,16] α-FeSe has a PbO-type structure, different from the NiAs-type structure which has been studied extensively in β-FeSe.[17,18] The crystal structure of α-FeSe is composed of stacked layers of edge-sharing $FeSe_4$ tetrahedra, and belongs to the space group $P4/nmm$. α-FeSe has been observed to distort from tetragonal to a triclinic structure below 105 K, while its analog α-FeTe, which is tetragonal at room temperature, transforms to an orthorhombic lattice at temperatures below 45 K. α-Fe(Se,Te) has a simpler structure than the different families of Fe-based superconductors, being essentially their infinite-layer analog. Among the consequences of this substantial structural difference are a shift of the SDW transition temperature by a factor of 2–3, to 65 K in Fe(Se,Te) from 140–200 K in the parent compounds of the FeAs systems. Further, the resistivity of Fe(Se,Te) shows a semiconductorlike temperature dependence, completely different from the metallic behavior of the FeAs-based materials. However, it is superconducting at temperatures up to 13 K for the composition $Fe_{1.03}Se_{0.3}Te_{0.7}$.[19] As a safer member of the family of iron-based superconductors, Fe(Se,Te) would seem destined to play an important role both in fundamental research into iron-based superconductivity and in its potential applications.

To date, the mechanism for superconductivity in the iron-based compounds remains unclear. Many theoretical scenarios, particularly a magnetic origin and electron-phonon coupling, have been proposed to understand the pairing mechanism. Further, the study of the SDW above T_c is tightly correlated with the structural properties. Thus a detailed study of the phonon modes in each series of Fe-based superconductors can be expected to yield important clues regarding all of the above aspects, and Raman scattering is well known to be a unique probe of zone-center optical phonons. Raman-scattering studies have so far been accomplished only for FeAs superconductors, and are reported in Refs. 20–22.

In this Rapid Communication, we report polarized Raman-scattering results obtained on $Fe_{1+y}Se_xTe_{1-x}$ single crystals, both for the $x=0$ parent compound and for the superconducting material with $x=0.30$. The zone-center optical modes were classified by a group-theoretical analysis and the Raman-active phonons assigned accordingly. We have performed first-principles lattice-dynamics calculations using both the relaxed and the experimental atomic positions, and find that the latter correspond more closely to the experimental measurements.

The single crystals used in the Raman-scattering experiments were prepared by the Bridgeman technique. Details of the crystal-growth process are presented elsewhere.[19] The exact compositions of the compounds studied here were estimated to be $FeTe_{0.92}$ and $Fe_{1.03}Se_{0.30}Te_{0.70}$. Raman-scattering measurements were performed with a triple Horiba Jobin Yvon T64000 spectrometer equipped with an optical microscope and liquid-nitrogen-cooled back-illuminated charge-coupled device (CCD) detector. A ×50 long-

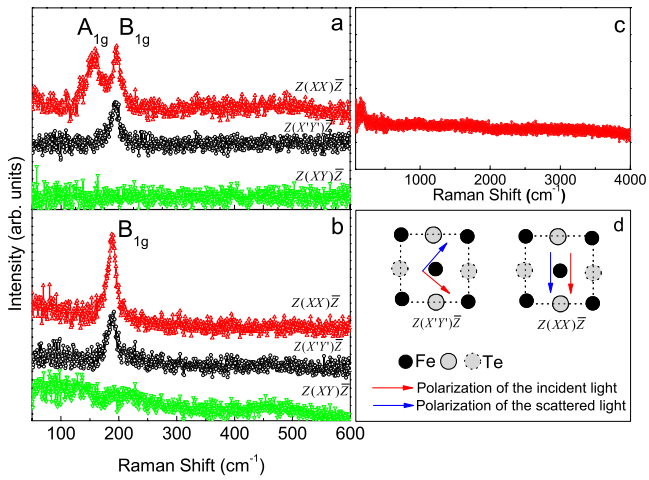

FIG. 1. (Color online) Room-temperature Raman spectra of (a) $FeTe_{0.92}$ and (b) $Fe_{1.03}Se_{0.3}Te_{0.7}$ for different polarized scattering geometries in the *ab* plane. (c) Extended spectrum of $FeTe_{0.92}$ in polarization configuration $Z(XX)\bar{Z}$. (d) Schematic illustration of two sample polarization configurations, $Z(XX)\bar{Z}$ and $Z(X'Y')\bar{Z}$ (see also Fig. 2).

working-distance objective was employed to focus the laser beam, with a wavelength of 532nm, into a spot of about 4 μm in diameter on the crystal surfaces, and to collect the scattered light. The crystals were cleaved and, to avoid possible contamination or decomposition in air, were placed immediately in a cryostat, which was evacuated to 3×10^{-6} Torr. The crystal surfaces are parallel to the *ab* plane, and Raman measurements were conducted on these flat surfaces. Because the samples are good metals and the crystal surfaces are perfect, most of the laser intensity was simply reflected back. The effective incident light intensity, and hence the Raman signal, was low, necessitating long acquisition times.

α-FeTe has space group $P4/nmm$. The Fe and Te atoms have respective Wyckoff positions 2*a* and 2*c*. The classification of the zone-center optical modes is similar to that of Ref. 20 for SmFeAsO and LaFeAsO, and thus is not reproduced in full detail here. By symmetry considerations, one may expect four Raman-active modes: A_{1g}(Te), B_{1g}(Fe), E_g(Te), and E_g(Fe); the E_g modes are twofold degenerate. Because the experiments are performed within the *ab* plane, it is easy to verify that the E_g modes are absent as a consequence of their Raman tensors. Both the A_{1g} and the B_{1g} mode should be present when the polarization configuration is $Z(XX)\bar{Z}$, while only the B_{1g} mode should remain when the configuration is changed to $Z(X'Y')\bar{Z}$. This expectation is verified clearly by the experimental observations shown in Fig. 1(a), where both the A_{1g} and B_{1g} modes of $FeTe_{0.92}$ are found to lie lower in frequency than the equivalent modes in $Sr_{1-x}K_xFe_2As_2$ single crystals.[22] By contrast, for $Fe_{1.03}Se_{0.3}Te_{0.7}$, the A_{1g} mode of Te is absent in all scattering geometries, as shown in Fig. 1(b). To explain this result, we note first that more impurities or vacancies may be introduced into the Se-doped samples because the growth conditions are quite critical for high-quality single crystals. Second, the requirements for phase formation dictate that the two samples have a small difference in stoichiometric ratio: specifically, $FeTe_{0.92}$ corresponds to $Fe_{1.09}Te$, while the Se-doped system is $Fe_{1.03}Se_{0.3}Te_{0.7}$. The excess Fe ions occupy Fe(2) positions, and may thus have a substantial effect on the vibration of neighboring Te ions. Finally, it is reasonable to expect that 30% Te substitution by Se may in itself suppress the Te vibration mode.

It is important to remark that a slight enhancement can be observed in the spectra of $Fe_{1.03}Se_{0.3}Te_{0.7}$ below 300 cm^{-1}. This may originate from electronic Raman scattering, and further measurements are required to identify definitively the nature of this feature. By contrast, there is no obvious feature at all in the high-energy spectra, which were measured up to 4000 cm^{-1} [Fig. 1(c)]. If it were present at these energies in the material, evidence of electron-phonon coupling would be expected in the extended spectra.

To compare with the observed phonon modes, we have calculated the nonmagnetic electronic structure and the zone-center phonons of α-FeTe within the framework of density-functional perturbation theory (DFPT). We applied the plane-wave basis method with the local (spin) density approximation for the exchange-correlation potentials,[23] while the generalized gradient approximation (GGA) of Perdew-Burke-Ernzerhof[24] was also tested without meaningful changes found. The ultrasoft pseudopotentials[25] were used to model the electron-ion interactions. After the full convergence test, the cutoffs of kinetic energy for the wave function and for the charge density were respectively 40 and 400 Ryd. Also the Gaussian smearing technique was performed on a uniform $24 \times 24 \times 12$ lattice of points in reciprocal space. We then employed the DFPT to generate the dynamical matrix, from which the phonon frequencies and atomic displacements were derived.

The $Fe_{1+y}Te$ compounds (PbO-type structure) have a narrow range of variation in y.[18] The experimental measurements show that the excess Fe atoms partially occupy the interstitial sites.[26] This makes first-principles calculations complicated because thousands of averages over sample disorder would be required, and for this reason it was necessary to neglect the excess Fe atoms in the phonon calculations, while the effect of different cell parameters (experimental and relaxed) on phonons is taken into account.

The cell parameters and calculated results are listed in Table I together with the experimental Raman data. It is worth emphasizing that the calculated results at zero temperature are compared to the results of Raman experiments performed at room temperature: this is because such a comparison ensures the same nonmagnetic structures in each case, as the ground state of $Fe_{1+y}Te$ compounds at low temperature is magnetically ordered. The temperature effect can be included by noting that if only the temperature is increased while the other properties of the sample (such as the magnetic state) are unchanged, the measured phonons should soften by an amount equivalent to the energy required for the same vibration at higher temperatures. In this way it is possible to evaluate the effects of temperature when assigning the phonon modes.

From Table I, the calculated phonon modes are completely consistent with the symmetry analysis. Qualitatively, all of the Raman-active modes were found and assigned ac-

TABLE I. Left: assignment of optical phonons in FeTe as deduced from first-principles calculations performed as part of this study; "NM-relaxed" and "NM-exp" refer to frequencies obtained from these calculations (see text), in units of cm^{-1}. Right: experimental and relaxed cell parameters. a, b, and c are the crystal axes, while Z denotes the Wyckoff positions in the c direction for the corresponding atoms.

Symmetry	Atoms	NM-relaxed	NM-exp	Expt.	Active	Cell parameter	Relaxed	Expt.
E_g	Te	73.3	59.1		Raman	Space group	$P4/nmm$	$P4/nmm$
A_{1g}	Te	181.1	140.3	159.1	Raman	a (Å)	3.7078	3.8123
E_u	Fe+Te	253.8	195.9		IR	b (Å)	3.7078	3.8123
E_g	Fe	283.0	196.9		Raman	c (Å)	6.0326	6.2515
B_{1g}	Fe	276.2	215.7	196.3	Raman	Z_{Fe}	0	0
A_{2u}	Fe+Te	321.2	250.6		IR	Z_{Te}	0.2704	0.2813

cording to the displacement patterns shown in Fig. 2. Quantitatively, the arrows in Fig. 2 indicate not only the vibration directions of the corresponding atoms but also, by their lengths, represent the relative vibration amplitudes compared with those of other atoms in the same mode. The calculated infrared phonon frequencies are also reported in Table I, but are not considered further here.

By comparison with the experimental Raman data, the nonmagnetic phonon calculations performed using relaxed cell parameters (denoted NM-relaxed in Table I) failed to provide a reasonable reproduction of the B_{1g} mode frequency of Fe, even when considering the effect of temperature. This behavior is quite unlike the case in previously reported phonon calculations on iron-based superconductors such as LaFeAsO, where the relaxed parameters always led to more accurate results.[21] We have also verified the calculated results using the experimental unit-cell parameters in combination with the energy-minimized internal Te positions (not shown here), which gives results similar to within frequency shifts of only 5 cm^{-1}. Quite generally, relaxation of the atomic positions balances the internal atomic forces in the unit cells, while relaxation of the unit-cell parameters further reduces the unit-cell stresses. The consistency of the phonon results for different ways of accomplishing this relaxation indicates that it is not the unit-cell stresses which are responsible for the discrepancies found when comparing with the experimental results. However, by using the experimental cell parameters (denoted NM-exp), the calculated B_{1g} mode frequency is found to be in quite good agreement with the experimental data. This implies that the excess of Fe atoms is affecting the steady-state atomic positions, and further evidence for their effects on the electronic properties has been obtained for $Fe_{1.076}Te$.[19] This may also be one of the reasons for the instability of the materials (below).

Finally, an interesting decomposition process is observed in the measurements. If the laser spot is held on a fixed point on the freshly cleaved surface of $Fe_{1.03}Se_{0.3}Te_{0.7}$ in vacuum for more than 3 h, the measured spectrum changes completely. The resulting spectrum is in fact quite similar to that obtained for $FeTe_{0.92}$ after exposure to air for several days (Fig. 3). The origin of this effect may be found in the results of Refs. 27 and 28, from which it is clear that the anomalous

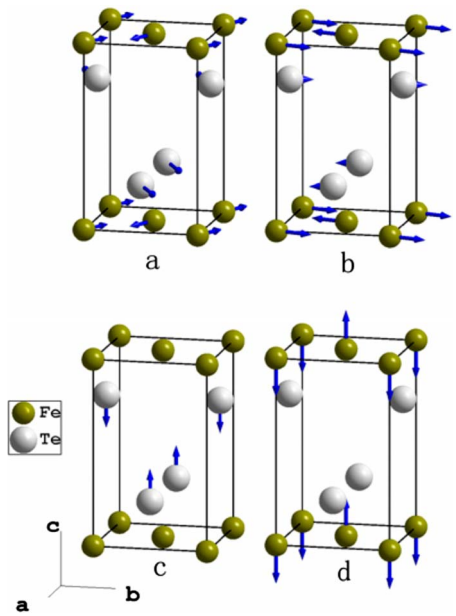

FIG. 2. (Color online) Displacement patterns for the Raman-active modes of α-FeTe, obtained from LDA calculations. [(a) and (b)] E_g modes, (c) A_{1g} mode of Te atoms, and (d) B_{1g} mode of Fe atoms.

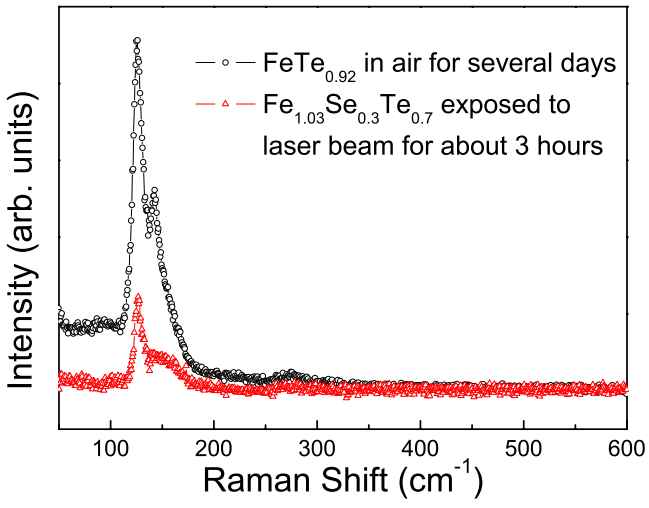

FIG. 3. (Color online) Room-temperature Raman-scattering spectra of the surface from samples exposed to air for several days and from one fixed point of the cleaved sample surface held under continuous laser irradiation. The polarization is $Z(XX)\bar{Z}$.

spectrum originates from amorphous Te.[27] Thus it is possible that $Fe_{1+y}Se_xTe_{1-x}$ is not stable in air, and that one of its decomposition products is amorphous Te rather than TeO_2. The decomposition may originate from its rather complicated phase diagram.[16,29] The decomposition of $Fe_{1+y}Se_xTe_{1-x}$ in air for long periods, and through irradiation for shorter periods, may restrict the potential applications of this system, and even some types of experimental study.

In conclusion, we have measured the room-temperature polarized Raman-scattering spectra of $FeTe_{0.92}$ and $Fe_{1.03}Se_{0.3}Te_{0.7}$ single crystals. We performed first-principles electronic band-structure calculations, and used these in combination with a symmetry analysis both to identify the phonon modes of α-FeTe and to compute their frequencies. When Te ions are partially substituted by Se ions in superconducting $Fe_{1.03}Se_{0.3}Te_{0.7}$, only the B_{1g} mode of the Fe atom can be observed, presumably due to the effect of random Te replacement by Se in destroying the periodic potential of the Te atoms. The frequency of the Fe B_{1g} mode is lower in the superconductor than in the parent compound α-FeTe. It is noteworthy to find that $Fe_{1+y}Se_xTe_{1-x}$ is not quite stable in air, one of the decomposition products being identified as amorphous Te. By providing detailed information on Raman phonons in FeTe-series superconductors, this work opens the way to further studies of the coupled structural, magnetic, and electronic properties of these systems.

We thank Bruce Normand for fruitful discussions and for a critical reading of the manuscript. This work was supported by the National Basic Research Program of China (Grants No. 2006CB9213001 and No. 2006CB601002) and by the NSFC (Grants No. 10574064 and No. 20673133).

*qmzhang@ruc.edu.cn

[1] Y. Kamihara, T. Watanabe, M. Hirano, and H. Hosono, J. Am. Chem. Soc. **130**, 3296 (2008).
[2] X. H. Chen, T. Wu, G. Wu, R. H. Liu, H. Chen, and D. F. Fang, Nature (London) **453**, 761 (2008).
[3] G. F. Chen, Z. Li, D. Wu, G. Li, W. Z. Hu, J. Dong, P. Zheng, J. L. Luo, and N. L. Wang, Phys. Rev. Lett. **100**, 247002 (2008).
[4] Z. A. Ren, G. C. Che, X. L. Dong, J. Yang, W. Lu, W. Yi, X. L. Shen, Z. C. Li, L. L. Sun, F. Zhou, and Z. X. Zhao, EPL **83**, 17002 (2008).
[5] H. H. Wen, G. Mu, L. Fang, H. Yang, and X. Y. Zhu, EPL. **82**, 17009 (2008).
[6] M. Rotter, M. Tegel, and D. Johrendt, Phys. Rev. Lett. **101**, 107006 (2008).
[7] G. F. Chen, Z. Li, G. Li, W. Z. Hu, J. Dong, P. Zheng, N. L. Wang, and J. L. Luo, Chin. Phys. Lett. **25**, 3403 (2008).
[8] K. Sasmal, B. Lv, B. Lorenz, A. M. Guloy, F. Chen, Y.-Y. Xue, and C.-W. Chu, Phys. Rev. Lett. **101**, 107007 (2008).
[9] N. Ni, S. L. Bud'ko, A. Kreyssig, S. Nandi, G. E. Rustan, A. I. Goldman, S. Gupta, J. D. Corbett, A. Kracher, and P. C. Canfield, Phys. Rev. B **78**, 014507 (2008).
[10] G. F. Chen, Z. Li, J. Dong, G. Li, W. Z. Hu, X. D. Zhang, X. H. Song, P. Zheng, N. L. Wang, and J. L. Luo, Phys. Rev. B **78**, 224512 (2008).
[11] X. C. Wang, Q. Q. Liu, Y. X. Lv, W. B. Gao, L. X. Yang, R. C. Yu, F. Y. Li, and C. Q. Jin, Solid State Commun. **148**, 538 (2008).
[12] M. J. Pitcher, D. R. Parker, P. Adamson, S. J. C. Herkelrath, A. T. Boothroyd, R. M. Ibberson, M. Brunelli, and S. J. Clarke, Chem. Commun. (Cambridge) (2008) 5918.
[13] J. H. Tapp, Z. Tang, B. Lv, K. Sasmal, B. Lorenz, P. C. W. Chu, and A. M. Guloy, Phys. Rev. B **78**, 060505(R) (2008).
[14] C. de la Cruz, Q. Huang, J. W. Lynn, J. Y. Li, W. Ratcliff, J. L. Zarestky, H. A. Mook, G. F. Chen, J. L. Luo, N. L. Wang, and P. C. Dai, Nature (London) **453**, 899 (2008).
[15] F. C. Hsu, J. Y. Luo, K. W. Yeh, T. K. Chen, T. W. Huang, P. M. Wu, Y. C. Lee, Y. L. Huang, Y. Y. Chu, D. C. Yan, and M. K. Wu, Proc. Natl. Acad. Sci. U.S.A. **105**, 14262 (2008).
[16] K. W. Yeh, T. W. Huang, Y. L. Huang, T. K. Chen, F. C. Hsu, P. M. Wu, Y. C. Lee, Y. Y. Chu, C. L. Chen, J. Y. Luo, D. C. Yan, and M. K. Wu, EPL **84**, 37002 (2008).
[17] P. Terzieff and K. L. Komarek, Monatsh. Chem. **109**, 651 (1978).
[18] W. Schuster, H. Mkiler, and K. Komarek, Monatsh. Chem. **110**, 1153 (1979).
[19] G. F. Chen, Z. G. Chen, J. Dong, W. Z. Hu, G. Li, X. D. Zhang, P. Zheng, J. L. Luo, and N. L. Wang, arXiv:0811.1489, Phys. Rev. B (to be published).
[20] V. G. Hadjiev, M. N. Iliev, K. Sasmal, Y.-Y. Sun, and C. W. Chu, Phys. Rev. B **77**, 220505(R) (2008).
[21] S. C. Zhao, D. Hou, Y. Wu, T.-L. Xia, A. M. Zhang, G. F. Chen, J. L. Luo, N. L. Wang, J. H. Wei, Z. Y. Lu, and Q. M. Zhang, Supercond. Sci. Technol. **22**, 015017 (2009).
[22] A. P. Litvinchuk, V. G. Hadjiev, M. N. Iliev, B. Lv, A. M. Guloy, and C. W. Chu, Phys. Rev. B **78**, 060503(R) (2008).
[23] P. Giannozzi *et al.* (http://www.quantum-espresso.org).
[24] J. P. Perdew, K. Burke, and M. Ernzerhof, Phys. Rev. Lett. **77**, 3865 (1996).
[25] D. Vanderbilt, Phys. Rev. B **41**, 7892 (1990).
[26] W. Bao, Y. Qiu, Q. Huang, M. A. Green, P. Zajdel, M. R. Fitzsimmons, M. Zhernenkov, M. Fang, B. Qian, E. K. Vehstedt, J. Yang, H. M. Pham, L. Spinu, and Z. Q. Mao, arXiv:0809.2058 (unpublished).
[27] A. S. Pine and G. Dresselhaus, Phys. Rev. B **4**, 356 (1971).
[28] A. S. Pine and G. Dresselhaus, Phys. Rev. B **5**, 4087 (1972).
[29] M. H. Fang, H. M. Pham, B. Qian, T. J. Liu, E. K. Vehstedt, Y. Liu, L. Spinu, and Z. Q. Mao, Phys. Rev. B **78**, 224503 (2008).